ISSN 0025-6544, Mechanics of Solids, 2020, Vol. 55, No. 5, pp. 643–653. © Allerton Press, Inc., 2020.
Russian Text © The Author(s), 2020, published in Izvestiya Rossiiskoi Akademii Nauk, Mekhanika Tverdogo Tela, 2020, No. 5, pp. 51–63.

Mechanics of Growing and Heat Treatment Processes of Monocrystalline Silicon

N. A. Verezub[a],* and A. I. Prostomolotov[a],**

[a] *Ishlinsky Institute for Problems in Mechanics, RAS, Moscow, 119526 Russia*

**e-mail: verezub@ipmnet.ru*

***e-mail: prosto@ipmnet.ru*

Received January 21, 2020; revised February 19, 2020; accepted April 4, 2020

Abstract—One of the urgent problems of mechanics is the study of the regularities of thermomechanical processes that affect the formation of microdefects in dislocation-free silicon single crystals both at the stage of their growth from the melt by the main industrial technology called the Czochralski method, and in subsequent heat treatment technologies of the wafers cut from them. This requires the development of coupled thermomechanical models both for the melt-crystal system, taking into account the crystallization process, and for the entire volume of the thermal unit of industrial growth plants, so that, taking into account the calculated "thermal history" of growing a particular silicon single crystal using modern models of defect formation, determine the regularities of the recombination and transfer processes. intrinsic point defects with their agglomeration into microdefects in monocrystalline silicon. This article provides a brief overview of the work carried out at IPMech RAS in this direction.

Keywords: single crystal growth, silicon, Czochralski method, intrinsic point defect, recombination, microdefect, diffusion, modeling, stress, deformation, heat treatment, plate

DOI: 10.3103/S0025654420300056

1. INTRODUCTION

Semiconductor silicon and the main technology of its growth by the method of directional crystallization from the Czochralski melt are the basis for the wide development of solid-state electronics. The components of the installation for growing silicon single crystals by the Czochralski method have axial symmetry. The setup for growing is shown in Fig. 1: *1* is the crystal, *2* is the melt, *3* is the crystallization front (CF), *4* is the crucible, *5* is the stand, *6* is the heater, *7* is the thermal insulation, *8* is the heat shield, *9* is the water-cooled body; overall dimensions: $H = 146$ cm and $D = 86$ cm. Cylindrical monocrystalline silicon ingots with a length of $L_k = 100–150$ cm and a diameter of 15 and 20 cm are pulled at a speed V from the bottom up from the melt contained in a graphite crucible surrounded by a high-temperature resistive heater, at In this case, the entire structure is placed in a water-cooled chamber and supplemented with thermal screens to control the temperature in the growing monocrystal. The crystal rotates with an angular velocity Ω_k, and the crucible with a stand rotates in the opposite direction with a velocity Ω_T.

The results of modeling of the thermomechanical processes serve as the basis for optimizing the designs of heating units, designing new installations, and are important in developing the parameters of thermal and speed parameters of growing. On their basis, practical recommendations are given for optimizing the designs of heat shields and heat-insulating elements, as well as thermal and dynamic conditions for the growth of single crystals. To effectively influence the axial temperature distribution in the growing single crystal, special designs of heat shields are used near the lateral surface of the crystal (for example, *8* in Fig. 1).

An important problem in the growth of dislocation-free single crystals is the problem of reducing the content and reducing the size of the microdefects present in them. Growth microdefects contained in wafers have a significant impact on the performance of integrated circuits. The main role in the formation of microdefects in single crystals grown by the Czochralski method is played by intrinsic point defects (vacancies and interstitial atoms). This necessitates theoretical and experimental studies on the influence of thermal and rate modes of growth on the nature, size, and distribution of microdefects in a single crys-

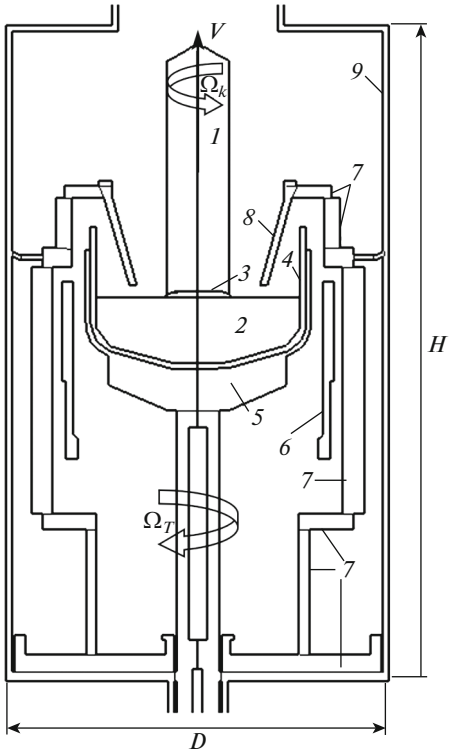

Fig. 1.

tal. Also, an important role is played by studies on the influence of various kinds of thermal effects on the behavior of microdefects in plates cut from a single crystal and on their strength characteristics.

The use of modern models and modeling methods forms the basis of the considered direction, which is being developed at IPMech RAS. The created mechanical and mathematical models are verified according to experimental data and are used to optimize the designs of thermal units of heavy industrial growth plants and temperature-dynamic conditions for growing single crystals and temperature-time modes of heat treatment of the plates, which guarantee control of the nature, content, size and distribution of microdefects in them [1–3].

2. MATHEMATICAL MODELING OF THERMAL PROCESSES IN INSTALLATIONS FOR GROWING SILICON SINGLE CRYSTALS

The basis of the conjugate mathematical model of heat transfer processes is the axisymmetric radiation-conductive calculation, which is realized by means of finite element approximations in a complex (non-simply connected) region with a significant role of thermal radiation from open surfaces [4]. Such a calculation allows to take into account the complex geometry and features of the technological parameters of a specific heating unit for growing silicon single crystals by the Czochralski method, for the example shown in Fig. 1.

The convection in the melt is taken into account on the basis of the conjugation of the radiation-conductive model and the model of conductive-convective processes in the crystal-melt system, taking into account the release of the latent heat of crystallization Q_H. For this, the temperature distributions obtained as a result of the calculation using the radiation-conductive model for the entire volume of the heating unit are set at the boundaries of the crystal and the melt.

The hydrodynamic model is constructed on the basis of the numerical solution of the full three-dimensional Navier – Stokes equations together with the equations of convective heat transfer in the melt due to rotation of the crystal and crucible, as well as thermal gravitational convection. The parameters of the hydrodynamic model are written in dimensionless form: $Re = \Omega_k R_k/\nu$ is the Reynolds number, $Ros = \Omega_k/\Omega_T$ is the Rossby number, $Gr = g\beta_T R_k^3 \Delta T/\nu^2$ is the Grashof number, $Pr = \nu/a$ is the Prandtl number. Here, R_k is the radius of the crystal, Ω_k, Ω_T are the angular velocities of rotation of the crystal and crucible,

Table 1

Material No. on Fig. 1	Density ρ, g/cm^3	Heat capacity C_p, J/g · K	Emissivity ε	Thermal conductivity λ, W/(m · K)
Silicon crystal, *1*	2.33	1.0	0.70	$-0.47 + 2.0 \times 10^{-4}T + 580/T$
Quartz crucible, *4*	2.2	1.24	0.85	0.04
Graphite rigging, *5–8*	1.74	1.0	0.80	$0.7587 - 4.8751 \times 10^{-4}T + 1.369 \times 10^{-7}T^2 - 1.6226 \times 10^{-11}T^3$
Steel case, *9*	8.0	0.5	0.45	0.15

Table 2

Material No. on Fig. 1	Density ρ, g/cm^3	Coef. thermal expansion β_T, K^{-1}	Thermal conductivity λ, W/m · K	Heat capacity C_p, J/g · K	Latent heat Q_H, J/g	Kinem. viscosity ν, cm^2/s
Silicon melt, *2*	2.53	1.1×10^{-4}	1.1	0.91	1804	0.003

ν is the kinematic viscosity of the melt, g is the acceleration of gravity, $\beta_T = -\rho^{-1}\partial\rho/\partial T$ is the coefficient of thermal expansion, ρ is density, ΔT is the maximum deviation of the temperature T from the crystallization temperature T_k.

An important role in the adequacy of such a conjugate calculation is played by the thermophysical parameters of the solid-state components (Table 1) and the silicon melt (Table 2), which are given with the number of the corresponding component of the thermal unit in Fig. 1.

Let us consider the simulation results for two stages of growing a silicon single crystal with a diameter of 20 cm and a length of 100 cm, corresponding to 10 and 30% of the length of the cylindrical part of the ingot L_k. In this case, it was assumed that there was no heat shield *8* shown in the diagram of the heating unit in Fig. 1.

Figure 2a shows the growth stage corresponding to the 10% length of the grown cylindrical part of the ingot. The rotation rates of the crystal and crucible corresponded to the following parameters: $Re = 6 \times 10^4$, $Ros = -0.446$, $Gr = 2 \times 10^9$. The flow structure is multi-vortex and time-varying. Splitting the flow into a series of vortices leads to a decrease in heat transfer from the crucible walls to the CF. The presence in the crucible center of a flow directed to the bottom is the reason for the W-shaped profile of the CF.

Figure 2b shows the picture of heat transfer in the melt at the stage corresponding to the 30% length of the cylindrical part of the ingot. Compared to the previous case, the crucible rotation speed was slightly increased (up to $Ros = 0.54$). Raising the crucible relative to the heater leads to a decrease in the effect of lateral heating and a decrease in the Grashof number to 1.7×10^9. In this case, the vortex adjacent to the side wall of the crucible grows larger due to the absorption of smaller vortices, which contributes to better heat transport from the crucible to the CF and more uniform heating of the central region of the melt. Such changes cause the formation of a concave CF shape.

The results of the calculation of the thermal field in the crystal are used in the subsequent calculation of defect formation processes based on the construction of a "thermal history" for a specific process of growing a silicon crystal. This implies obtaining analytical expressions for the thermal field in the crystal $T(t, r, z)$ at any moment of time and for any point of the growing crystal, taking into account the shape of the CF. For this purpose and due to the fact that thermal processes are fast enough, the entire growth process is represented as a sequence of N independent stationary stages. The geometric parameters varying in the growth process, which have a significant effect on heat transfer in the thermal unit and on the change in the thermal field in the crystal, are the position of the crucible assembly, the height of the melt in the crucible, and the length of the crystal. The heater power and the crystal pulling speed V are also variable according to the preset programs.

The methodological approach [5] allows memorizing and storing temperature fields ("thermal history" of single crystal growth) for the entire growth process. Its essence consists in representing the temperature distributions along the axis and the edge of the crystal in the form of polynomials of high (6–8th) degree. They are calculated from the temperature fields in the crystal for each calculated growth stage

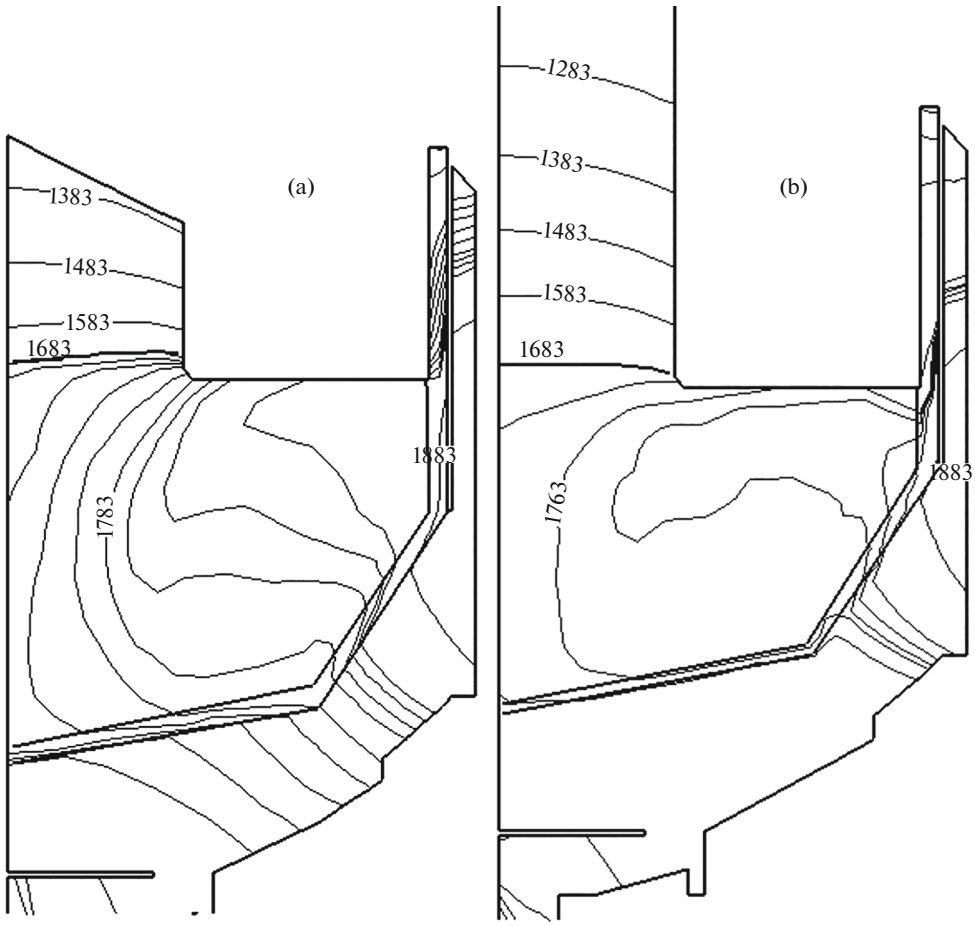

Fig. 2.

(altogether for $N \sim 20$ stages). Further, in mathematical models for calculating defect formation, these polynomials are specified as equation parameters (see the next section).

The temperature distribution in the growing single crystal plays an important role in the processes of defect formation. Therefore, a special heat shield *8*, shown in Fig. 1, is added to the standard design of the heating unit for the Czochralski method. With this screen, it is possible to influence the temperature field in the growing single crystal. A significant effect of the heat shield on the temperature field in a growing single crystal with a diameter of 20 cm and a length of a cylindrical part of 60 cm can be seen from a comparison of the isotherm patterns in a single crystal grown without the shield (a) and with the shield (b), shown in Fig. 3.

It is important to note that during the growth process in a single crystal, four characteristic thermal zones are distinguished, for each of which different models of defect formation are used:

1—near the CF at 1683 K, point defects (vacancies v and interstitial atoms i) are recombined, temperature gradients near the CF determine the residual concentration of vacancies and interstitial atoms after their recombination;

2—at 1373–1323 K, micropores and clusters of interstitial silicon atoms are formed, the size and concentration of growth microdefects are formed;

3—at 1223–1023 K, the oxygen solid solution decomposes with the migration of centers of nucleation of oxide defects (precipitates);

4—at 1023–723 K the sizes of precipitates grow and the final picture of microdefects in a single crystal is formed.

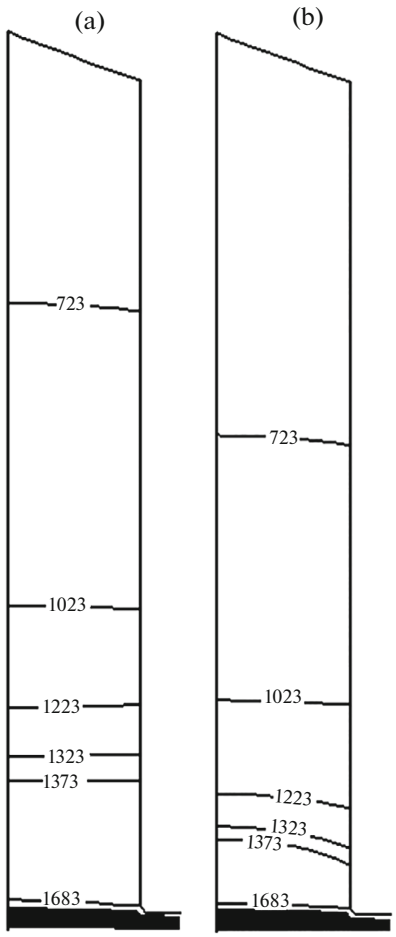

Fig. 3.

3. MODELING OF DEFECT FORMATION PROCESSES IN SILICON SINGLE CRYSTALS AND PLATES

The next step in coupled mathematical modeling is the use of the "thermal history" of the grown single crystal to calculate the defect formation processes in different temperature zones of the growing silicon single crystal (see Section 2). Let us consider the sequence of these calculations using the example of the "thermal history" of growing silicon single crystals with a diameter of 150 mm.

In temperature zone 1, the process of recombination of intrinsic point defects occurs (see Section 2). The annihilation of vacancies and interstitial atoms near the CF largely determines their subsequent migration and distribution in the crystal. The annihilation rate is equal to the difference between the rates of the forward recombination reaction and the reverse reaction of thermal generation of pairs of intrinsic point defects. The rate of the direct (binary) recombination reaction is proportional to the product of the concentration of point defects during their interaction. The speed of the back reaction is related to the speed of the forward reaction by the law of mass action.

In a silicon crystal grown by the Czochralski method, the transfer of vacancies and interstitial atoms is carried out mainly by convective diffusion, the process of thermal diffusion is neglected [6].

As an example, Fig. 4, a section of a grown single crystal near the crystallization front with a length of $l = 23$ cm and a radius of $r = 7.5$ cm is considered, for which the isolines $C_{iv} = C_i - C_v$ [10^{-12} cm^{-3}] of

Table 3

Material No. on Fig. 1	Poisson coef. μ	Thermal expansion coef. β_T, K^{-1}	Elastic modulus E, Pa
Silicon crystal, *1*	0.25	5.2×10^{-6}	$1.73 \times 10^{11} - 1.40 \times 10^{7} T$

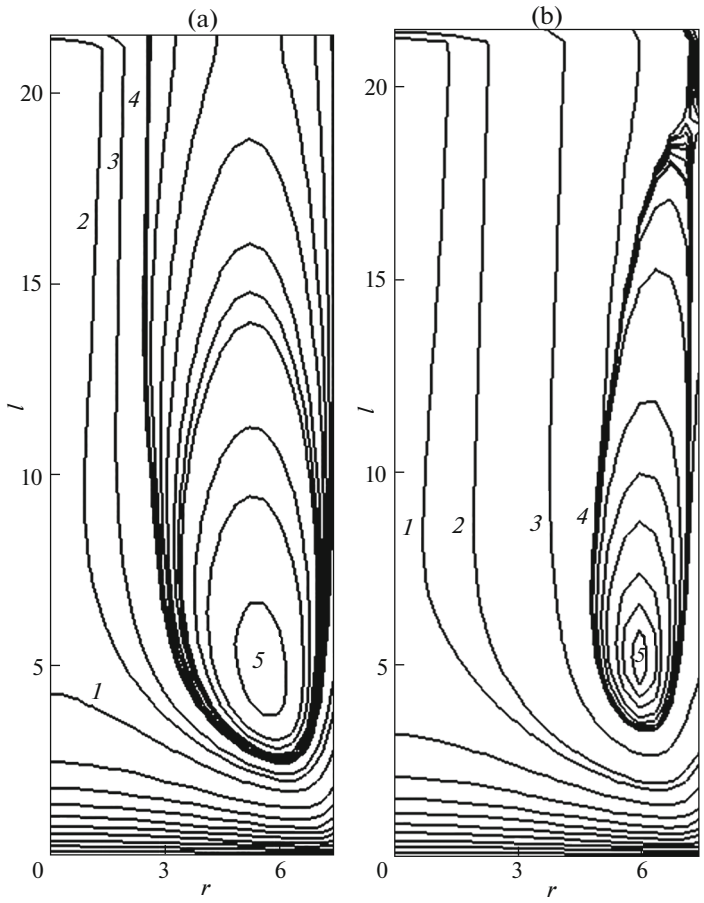

Fig. 4.

residual intrinsic point defects are shown (where C_i, C_v are the concentrations of interstitial atoms and vacancies) after their recombination in a silicon single crystal in two modes: (a) vacancy: *1*—20.0, *2*—16.0, *3*—4.5, *4*—0.1, *5*—2.7; (b) mixed (vacancy-interstitial): *1*—16.0, *2*—7.8, *3*—4.5, *4*—0.1, *5*—8.6. The differences are caused by different ratios between the pulling rate V and the axial temperature gradient on the CF.

In case (a), the concentration of residual vacancies is significant, since the pulling rate is high. However, as it decreases, the concentration of interstitial atoms increases, and at a certain value of V, the vacancy region narrows to the center of the crystal with the expansion of the interstitial region adjacent to its lateral surface (b). The radial distributions of the concentration of vacancies and interstitial atoms at the upper boundary of the computational domain characterize their residual values, which are the initial data for calculating the process of their agglomeration into microdefects in the colder temperature zone 2.

In temperature zone 2, to simulate the formation of growth micro-defects, both the ingot cooling rates and the concentration of residual intrinsic point defects after recombination are required. The mathematical model [5] takes into account the two-dimensionality of the thermal field in the crystal and the diffusion of vacancies.

Figure 5 shows the radial distributions of the density N_v, N_p [cm^{-3}] and the sizes of micropores R_v, R_p [nm] (a) and oxide particles (b) for a growing crystal with a radius of $r = 7.5$ cm and a length of $l = 0.3L_k$ grown in a mixed vacancy interstitial mode (here solid lines correspond to density, dotted line to defect sizes).

The maximum concentration of micropores reaches the value $N_v = 5 \times 10^4$ cm^{-3}, their size is $R_v =$ 23 nm within the central ring with a radius of 3 cm (a). The maximum concentration of oxide particles reaches a higher value: $N_p = 10^7$ cm^{-3}, and their size is much smaller: $R_p = 4.2$ nm within the central ring with a radius of 4 cm. Modeling of the formation of interstitial clusters is carried out using a similar scheme. They are located near the side surface of the silicon ingot. Estimates show that the values of their maximum density and radius are approximately 8×10^4 cm^{-3} and 54 nm.

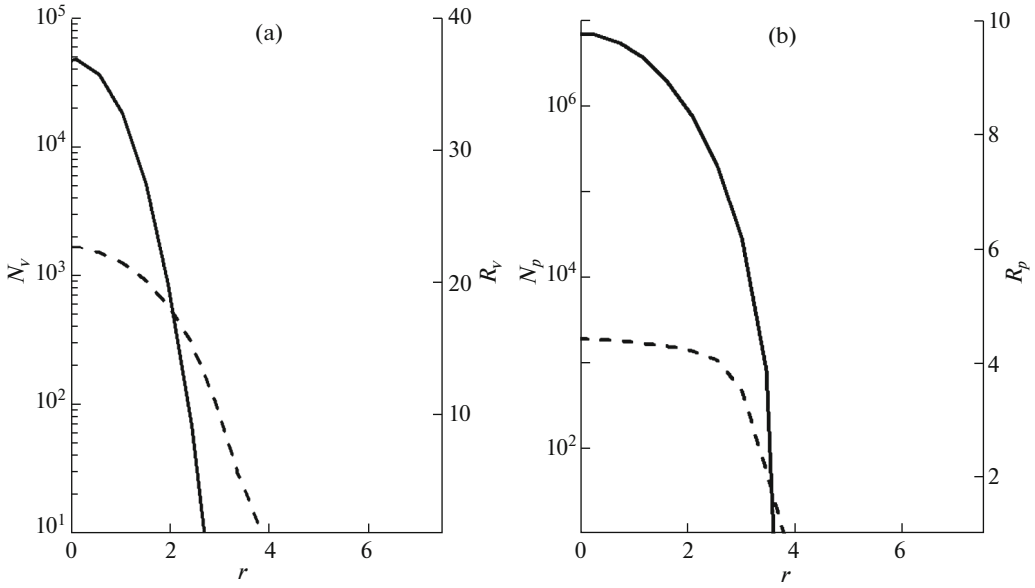

Fig. 5.

The results of calculations of the spatial distribution of microdefects were compared with the corresponding experimental data. To this end, it was necessary to present the calculated distributions of microdefects in the form of two-dimensional patterns of isolines for the entire length of the grown single-crystal ingot, i.e. all calculated stages of the growing process.

For a silicon single crystal grown under conditions corresponding to the calculations performed, a longitudinal cut of the ingot was made and the "lifetime" of electric carriers, the main empirical parameter of the quality of a single crystal, which characterizes the type and level of microdefects contained in it, was measured along its length. The maximum "lifetime" corresponds to the contour of the boundary between vacancy and interstitial microdefects.

A change in the pulling rate of a single crystal during the growth process significantly affects the distribution of microdefects. Figure 6 shows the change in the pulling rate V [mm/min] as a function of the relative length of the grown crystal l/L_k (a), which agrees with the distribution of the calculated isolines of microdefects (b) and the experimental map of the "lifetime" of electrical carriers (c). This can be seen by the coincidence of the calculated and measured contours of the boundary of vacancy and interstitial microdefects (see the dotted arrows pointing to this boundary). Spatial narrowing and expansion of the contour of this boundary are consistent with the change in the pulling speed.

The verification of the results of mathematical modeling was also carried out for silicon wafers cut from the grown single crystals [7]. These plates undergo high-temperature heat treatment in special thermal furnaces with lamp heating. The process consists of rapid heating of the plate to 1523 K, short-term holding (10–15 s) of the plate at this temperature, and then its rapid cooling to 823 K. As a result of heat treatment, a decrease in volumetric inhomogeneity and the level of microdefects is achieved. The use of the conjugate mathematical model considered above made it possible to calculate the spatio-temporal changes in the temperature field in the silicon wafer and, in accordance with these data, to calculate the process of diffusion and recombination of point defects. To verify the calculation results, the bulk density of oxygen precipitates was measured, according to which the profile of the vacancy concentration C_v over the plate thickness was constructed. Its comparison with a similar calculated profile of the vacancy concentration showed good agreement [8].

4. MODELING THE STRESS STATE IN SILICON SINGLE CRYSTALS

The presence of ultra-high stresses is an urgent problem for the technology of growing silicon single crystals with a diameter of 40 cm and a length of more than 100 cm, for the solution of which special supporting devices are proposed in the upper conical region where the crystal ingot is attached [9].

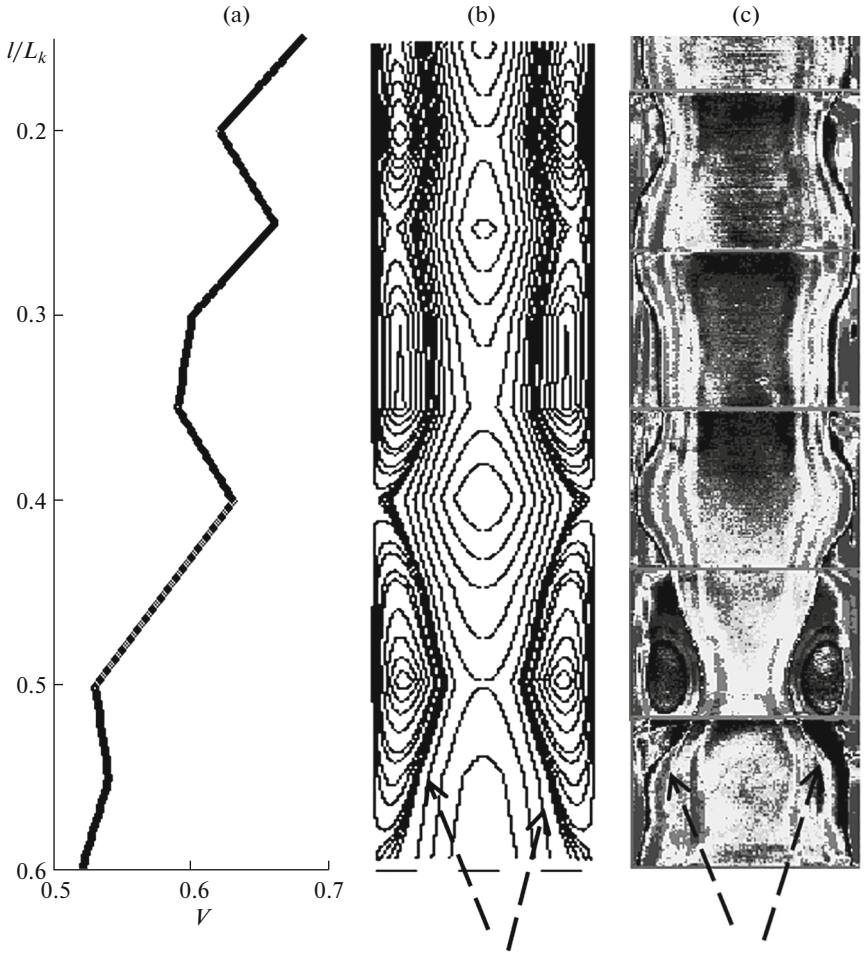

Fig. 6.

However, at smaller diameters, the most urgent is the analysis of the thermally stressed state of the grown single crystal, in particular, in the regions of the greatest axial and radial gradients that arise near the CF. For a silicon single crystal 10 cm in diameter and 40 cm in length, the calculations were performed in the thermoelastic approximation. Figure 7 shows the pictures of stress isolines according to the von Mises criterion calculated in accordance with the parameters given in Table 3. Their maximum values - 6.5 MPa are achieved on the lateral surface of the crystal near the CF, which is due to the presence of the largest temperature gradients in this region. With distance from the CF, the stresses decrease rapidly.

5. MODELING THE STRESS STATE IN SILICON PLATES

Optimization of the heat treatment modes of silicon wafers allows avoiding the appearance of dislocations and structural defects also in the post-growth period. For example, the results of calculating the three-dimensional stress state of silicon plates become very relevant for their large diameters of ~20 and 30 cm.

For the process of high-temperature processing with horizontal fastening of thin plates (~1000 μm thick) on three supports, such calculations were performed taking into account the crystallographic orientation (Fig. 8a: *1* is the silicon plate, *2* is the plate fastening on a ring support).

In [10], the influence of the shape and material of the plate supports, as well as their spatial arrangement, on the shear stresses along the possible spatial systems of dislocation slip in the silicon crystal lattice was analyzed. To identify dislocation-hazardous slip planes, the plate deflection was calculated along the action of gravitational forces for a given arrangement and thickness of the supports.

It was found that stresses according to the von Mises criterion σ [MPa] reach maximum values in the area of contact between the plate and the support (Fig. 8b), and the plates are the least stressed when the

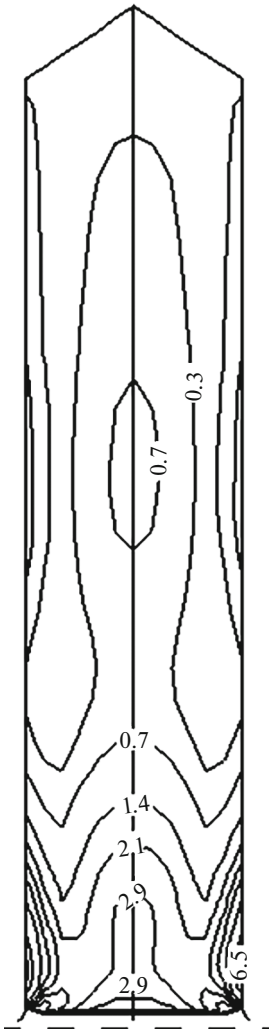

Fig. 7.

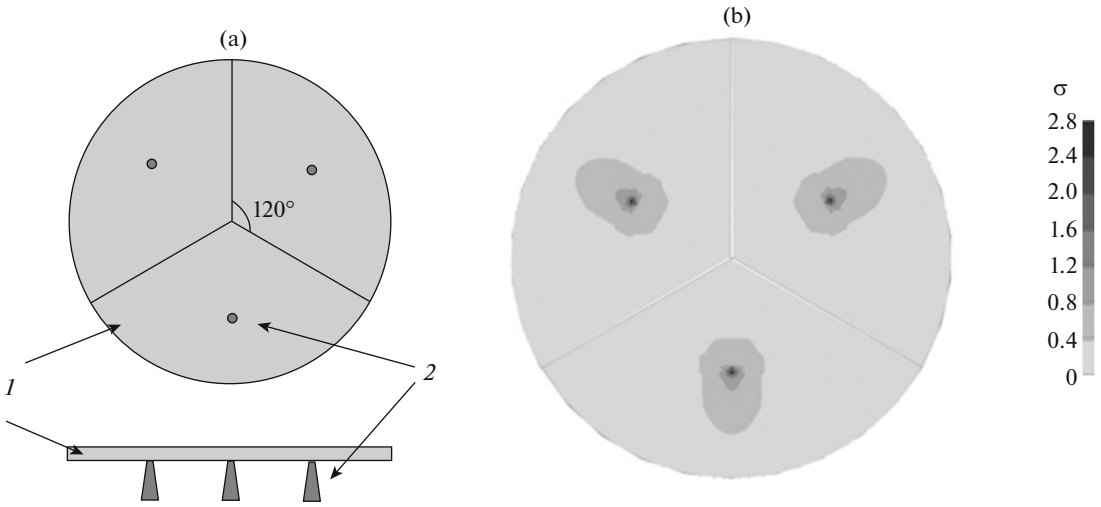

Fig. 8.

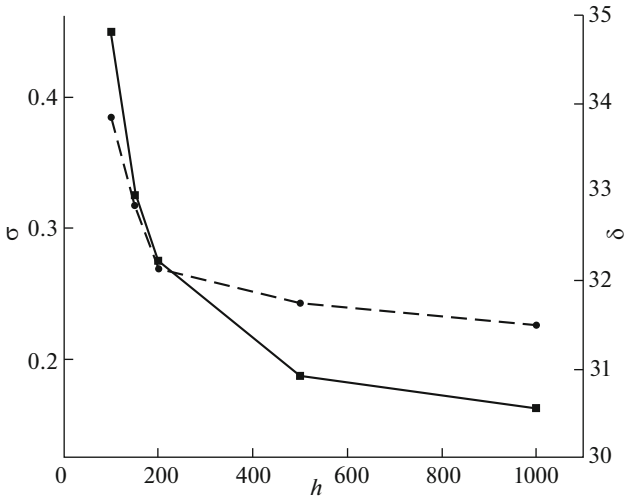

Fig. 9.

supports are located at a distance of $0.7R$ from the center of the plate, where R is the radius of the plate. For plates with a diameter of 20 cm, the values of the maximum stresses are approximately 2 times less than for plates with a larger diameter of 30 cm.

An increase in the plate diameter to 30 cm causes an increase in the values of maximum deformations by about 4.5 times. For this case, Fig. 9 shows the graphs of the maximum stress σ [MPa] and the bending of the plate δ [μm] depending on the width of the annular support h [μm] at a distance of $0.7R$ from the center of the plate.

Taking these results into account is necessary to reduce stresses in the plates in order to ultimately ensure the conditions for the formation of a practically defect-free working layer in the plates.

CONCLUSIONS

Coupled mechanical and mathematical models of heat transfer and defect formation were developed as applied to technologies for growing dislocation-free silicon single crystals by the Czochralski method and to the technology of high-temperature heat treatment of plates cut out of them. The possibilities of the developed models in the optimization of the thermal field in heating units for growing single crystals and in installations for high-temperature heat treatment of silicon plates were shown. The possibilities of controlling the thermally stressed state and defect formation during the growth and heat treatment of single-crystal dislocation-free silicon were analyzed.

FUNDING

The work was carried out on the computing base of the IPMech RAS (theme no. AAAA-A20-120011690136-2) with the support of the RFBR grant no. 18-02-00036.

REFERENCES

1. I. D. Epimakhov, M. V. Kutsev, V. P. Prisyazhnyuk, and A. I. Prostomolotov, "Growing silicon single crystals in the EKZ-1600 installation. Modeling the heat transfer process," Elektron. Prom., No. 3, 15–17 (2003).
2. N. A. Verezub, M. G. Mil'vidskiĭ, and A. I. Prostomolotov, "Heat transfer in installations for growing silicon monocrystals by the Czochralski method," Materialoved., No. 3, 2–6 (2004).
3. N. A. Verezub and A. I. Prostomolotov, "Modeling of the features of three-dimensional heat transfer and defect formation during dislocation-free large diameter single crystal growth by the Czochralski method," Izv. Vyssh. Uchebn. Zav. Mater. Elektron. Tekhn., No. 1, 4–10 (2007).
4. N. A. Verezub and A. I. Prostomolotov, "Investigation of heat transfer in the growth node of the Czochralski process based on the conjugate mathematical model," Izv. Vyssh. Uchedn. Zav. Mater. Elektron. Tekhn., No. 3, 28–34 (2000).

5. A. I. Prostomolotov, N. A. Verezub, and V. V. Voronkov, "Modeling of grown-in microdefect formation in large diameter dislocation-free silicon single crystals," Izv. Vyssh. Uchebn. Zav. Mater. Elektron. Tekhn., No. 2, 48–53 (2005).
6. N. A. Verezub, V. V. Voronkov, M. G. Mil'vidskiĭ, and A. I. Prostomolotov, "Interaction of intrinsic point defects during the growth of silicon monocrystals by the Czochralski method," Poverkhn. Rentgen. Sinkhron. Neitron. Issled., No. 10, 15–20 (2001).
7. N. A. Verezub, A. I. Prostomolotov, M. V. Mezhennyi, et al., "Theoretical and experimental study of the formation of grown-in and as-grown microdefects in dislocation-free silicon single crystals grown by Czochralski method," Crystallogr. Rep. **50** (Suppl. 1), S159-S167 (2005).
8. A. Prostomolotov, N. Verezub, M. Mezhennyi, and V. Resnik, "Thermal optimization of Cz bulk growth and wafer annealing for crystalline dislocation-free silicon," J. Cryst. Growth **318,** 187–192 (2011).
9. T. Iida, N. Machida, N. Takase, et al., "Development of crystal supporting system for diameter of 400mm silicon crystal growth," J. Cryst. Growth **229,** 31–34 (2001).
10. M. V. Mezhennyi, M. G. Mil'vidskii, and A. I. Prostomolotov, "Simulation of the stresses produced in large-diameter silicon wafers during thermal annealing," Phys. Solid State **45**, 1884–1889 (2003).

Translated by M. Katuev